Original Article

Comparative effect of skeletal stem cells versus bone marrow mesenchymal stem cells on rotator cuff tendon-bone healing

Linfeng Wang [a,b,c,d,1], Changbiao Guan [a,b,c,d,1], Tao Zhang [a,b,c,d], Yongchun Zhou [f], Yuqian Liu [a,b,c,d], Jianzhong Hu [b,c,d,e], Daqi Xu [a,b,c,d,**], Hongbin Lu [a,b,c,d,*]

[a] Department of Sports Medicine, Xiangya Hospital, Central South University, Changsha, 410008, Hunan Province, China
[b] Key Laboratory of Organ Injury, Aging and Regenerative Medicine of Hunan Province, Changsha, 410008, Hunan Province, China
[c] Hunan Engineering Research Center of Sports and Health, Changsha, 410008, Hunan Province, China
[d] National Clinical Research Center for Geriatric Disorders, Xiangya Hospital, Central South University, Changsha, 410008, Hunan Province, China
[e] Department of Orthopedics, Xiangya Hospital, Central South University, Changsha, 410008, Hunan Province, China
[f] Department of Spine Surgery, The Fourth Hospital of Changsha, Changsha Hospital of Hunan Normal University, Changsha, 410006, Hunan Province, China

ARTICLE INFO

ABSTRACT

Background: Bone marrow mesenchymal stem cells (BMSCs) have immense potential in applications for the enhancement of tendon-bone (T-B) healing. Recently, it has been well-reported that skeletal stem cells (SSCs) could induce bone and cartilage regeneration. Therefore, SSCs represent a promising choice for cell-based therapies to improve T-B healing. In this study, we aimed to compare the therapeutic potential of SSCs and BMSCs for tendon-bone healing.

Methods: SSCs and BMSCs were isolated by flow cytometry, and their proliferation ability was measured by CCK-8 assay. The osteogenic, chondrogenic, and adipogenic gene expression in cells was detected by quantitative real-time polymerase chain reaction (qRT-PCR). C57BL/6 mice underwent unilateral supraspinatus tendon detachment and repair, and the mice were then randomly allocated to 4 groups: control group (tendon-bone interface without any treatment), hydrogel group (administration of blank hydrogel into the tendon-bone interface), hydrogel + BMSCs group (administration of hydrogel with BMSCs into the tendon-bone interface), and hydrogel + SSCs group (administration of hydrogel with SSCs into the tendon-bone interface). Histological staining, Micro-computed tomography (Micro-CT) scanning, biomechanical testing, and qRT-PCR were performed to assay T-B healing at 4 and 8 weeks after surgery.

Results: SSCs showed more cell proportion, exhibited stronger multiplication capacity, and expressed higher osteogenic and chondrogenic markers and lower adipogenic markers than BMSCs. In vivo assay, the SSCs group showed a better-maturated interface which was characterized by richer chondrocytes and more proteoglycan deposition, as well as more newly formed bone at the healing site and increased mechanical properties when compared to other there groups. qRT-PCR analysis revealed that the healing interface in the SSCs group expressed more transcription factors essential for osteogenesis and chondrogenesis than the interfaces in the other groups.

Conclusions: Overall, the results demonstrated the superior therapeutic potential of SSCs over BMSCs in tendon-bone healing.

The translational potential of this article: This current study provides valuable insights that SSCs may be a more effective cell therapy for enhancing T-B healing compared to BMSCs.

---

* Corresponding author. Xiangya Hospital, Central South University, No. 87, Xiangya Road, Kaifu District, Changsha, 410008, Hunan Province, China.
** Corresponding author. Xiangya Hospital, Central South University, No. 87, Xiangya Road, Kaifu District, Changsha, 410008, Hunan Province, China.
E-mail addresses: Xudaqi96215@csu.edu.cn (D. Xu), hongbinlu@csu.edu.cn (H. Lu).
[1] The two authors contributed equally to this study

1. Introduction

Tendon-bone interface (TBI) or tendon enthesis connects two dramatically distinct tissues to transfer mechanical force between tendon/ligament and bone for facilitating movement [1–3]. Histologically, TBI could be categorized into a transitional series of tissue zones: tendon/ligament, uncalcified fibrocartilage, calcified fibrocartilage, and bone [4,5]. As a mechanical load-bearing tissue, TBI is highly prone to injury, and injured TBI is not effectively restored to its original structure because of bone loss at the healing site and limited regenerative ability of the fibrocartilage layer [6–8]. In contrast, mechanically weaker fibrovascular tissue accumulates at the repaired interface for obstructing the insertion of the tendon/ligament into the bone [9,10]. Thus, how to achieve the anatomical and functional restoration of injured TBI has been a hot research topic in sports medicine.

Cell-based therapies using stem cells represent a promising treatment choice for the enhancement of tendon-bone (T-B) healing [11–13]. Mesenchymal stem cells (MSCs), non-hematopoietic multipotent stem cells, have the ability to self-renew and differentiate into established cell types such as chondrocytes, osteoblasts, and adipocytes. MSCs could be obtained from a series of tissues, like bone marrow, adipose tissue, tendon, and synovium [14,15]. It is worth noting that BMSCs are the first discovered and the most widely used MSCs to promote T-B healing [16–18]. At present, SSCs have been extensively discovered in skeletal tissues and are known for their self-renewal ability and higher multi-differentiation potency specialized for bone/cartilage than any other stem cells [19,20]. However, SSCs typically do not demonstrate a significant propensity for differentiating into fat cells. Some studies have shown that SSCs can be activated by bone, cartilage, and TBI injuries, leading to enhanced biological behavior. Additionally, the transplantation of SSCs to the site of injury has been found to significantly promote the regeneration of bone and cartilage [21–23]. While the therapeutic effectiveness of SSCs in bone and cartilage regeneration has been extensively studied, their potential for treating TBI injuries has not been reported yet.

Identifying the optimal type of stem cells is crucial for the enhancement of T-B healing. To date, increased kinds of stem cells have been proven to have a greater ability to induce chondrogenesis and osteogenesis than BMSCs [24,25]. In the present study, we aimed to explore whether SSCs were more effective treatment to augment T-B healing as compared to BMSCs.

2. Methods

2.1. Isolation and culture of primary cells

Mouse BMSCs were isolated and cultured as described previously [26,27]. Briefly, bone marrow was flushed out from the bone marrow cavity of the left tibia and femur of 1-week-old C57BL/6 mice, and then centrifuged to collect bone marrow cells. These cells were mixed with red blood cell lysis buffer (Solarbio, Beijing, China), centrifuged, and then stained at 4 °C for 30 min with the following antibodies: Sca-1, CD29, CD45, and CD11b. Sca-1 antibodies were purchased from BD Bioscience (New Jersey, USA), and the others were purchased from BioLegend (California, USA). DAPI staining solution (BD bioscience) was used to label and exclude any dead cells. Next, the DAPI$^-$ CD45$^-$ CD11b$^-$ Sca-1$^+$ CD29$^+$ lived BMSCs were sorted out by flow cytometry and cultured with α-MEM (Procell, Wuhan, China) containing 10 % FBS, 1 % penicillin/streptomycin in a humidified atmosphere of 5 % CO$_2$ at 37 °C.

Mouse SSCs were isolated and cultured according to a previously established protocol [23,28]. The right tibia and femur of the above mice were minced and digested in collagenase with DNase at 37 °C for 30 min under gentle agitation. All dissociated cells were mixed with red blood cell lysis buffer, centrifuged, and then stained at 4 °C for 30 min with the following antibodies: CD45, Ter119, TIE2, THY1.1, THY1.2,

6C3, IGTAV, CD105 and CD200, all were purchased from BioLegend. DAPI staining solution was used to label and exclude any dead cells. DAPI$^-$ CD45$^-$ Ter119$^-$ TIE2$^-$ THY$^-$ 6C3$^-$ CD105$^-$ IGTAV$^+$ CD200$^+$ lived SSCs were sorted out by flow cytometry and cultured with α-MEM containing 10 % FBS, 1 % penicillin/streptomycin at 37 °C in a 5 % CO$_2$ incubator.

The sorted cells were designated as passage 0. When they reached 80 % confluence, the cells were sub-cultured, leading to an increase in their culture passage to passage 1.

2.2. Proliferation assay

The proliferative capacity of BMSCs and SSCs at passage 1 was evaluated using a cell counting Kit-8 reagent (CCK8, biosharp, Guangzhou, China) according to the manufacturer's instructions. In brief, cells (2×10^3 per well) were seeded into a 96-well culture plate and cultured at 37 °C, 5 % CO2. From days 1–7, cells were treated with a 1:10 mix of culture media (α-MEM containing 10 % FBS, 1 % penicillin/ streptomycin) and CCK-8 for 2 h at 37 °C, and the absorbance of each well was measured at 450 nm using a microplate reader (Bio-Rad 680, Hercules, USA).

2.3. Quantitative real-time polymerase chain reaction (qRT-PCR)

Total RNA of different differentiated cells and supraspinatus tendon (ST) enthesis was isolated using Trizol reagent (Invitrogen, Carlsbad, USA). Then, cDNA was synthesized by reverse transcription of 1 μg total RNA using the NovoScript® Plus All-in-one 1st Strand cDNA Synthesis SuperMix (gDNA Purge) (Novoprotein, Beijing, China). qRT-PCR was performed on QuantStudio™ 7 Flex Real-Time PCR Systems (Applied Biosystems, USA) with NovoStart® SYBR High-Sensitivity qPCR Super-Mix (Novoprotein, Beijing, China). Relative expression of mRNA was calculated using the $2^{-\Delta\Delta CT}$ method and normalized to β-actin. All details of the primers employed in the current study were listed in Table S1.

2.4. Animal experiment and group management

A total of 224 specific pathogen-free (SPF) male C57BL/6 mice underwent unilateral ST detachment and repair in their left shoulder according to a previously reported protocol [29]. The surgical procedure was briefly depicted in Fig. S1. After surgery, the mice were then randomly allocated to 4 groups: control group (tendon-bone interface without any treatment, n = 56), hydrogel group (administration of blank hydrogel (VitroGel Hydrogel Matrix, The Well Bioscience, New Jersey, USA) into the tendon-bone interface, n = 56), hydrogel + BMSCs group (administration of hydrogel with 1×10^5 BMSCs into the tendon-bone interface, n = 56), and hydrogel + SSCs group (administration of hydrogel with 1×10^5 SSCs into the tendon-bone interface, n = 56) (Fig. S2). According to experimental grouping, the hydrogel was combined with PBS containing 3 % BSA, either with or without passage 3 cells, at a 1:1 (v/v) ratio. Subsequently, 5 μl of the prepared hydrogel was placed into the tendon-bone interface after it reached a gel state at microsyringe needle. At postoperative weeks 4 and 8, the shoulder specimens including supraspinatus muscle, tendon, and humerus were collected to evaluate the healing quality of TBI by histological, radiographic, and biomechanical analysis. Furthermore, ST enthesis tissues, encompassing a 1-mm section of the tendon and the portion of the humeral head proximal to the growth plate near the site of tendon insertion, were meticulously harvested using microscissors under a microscope for qRT-PCR analysis to detect the expression of osteogenic and chondrogenic genes.

2.5. Histological staining

The shoulder specimens were fixed in the 4 % paraformaldehyde,
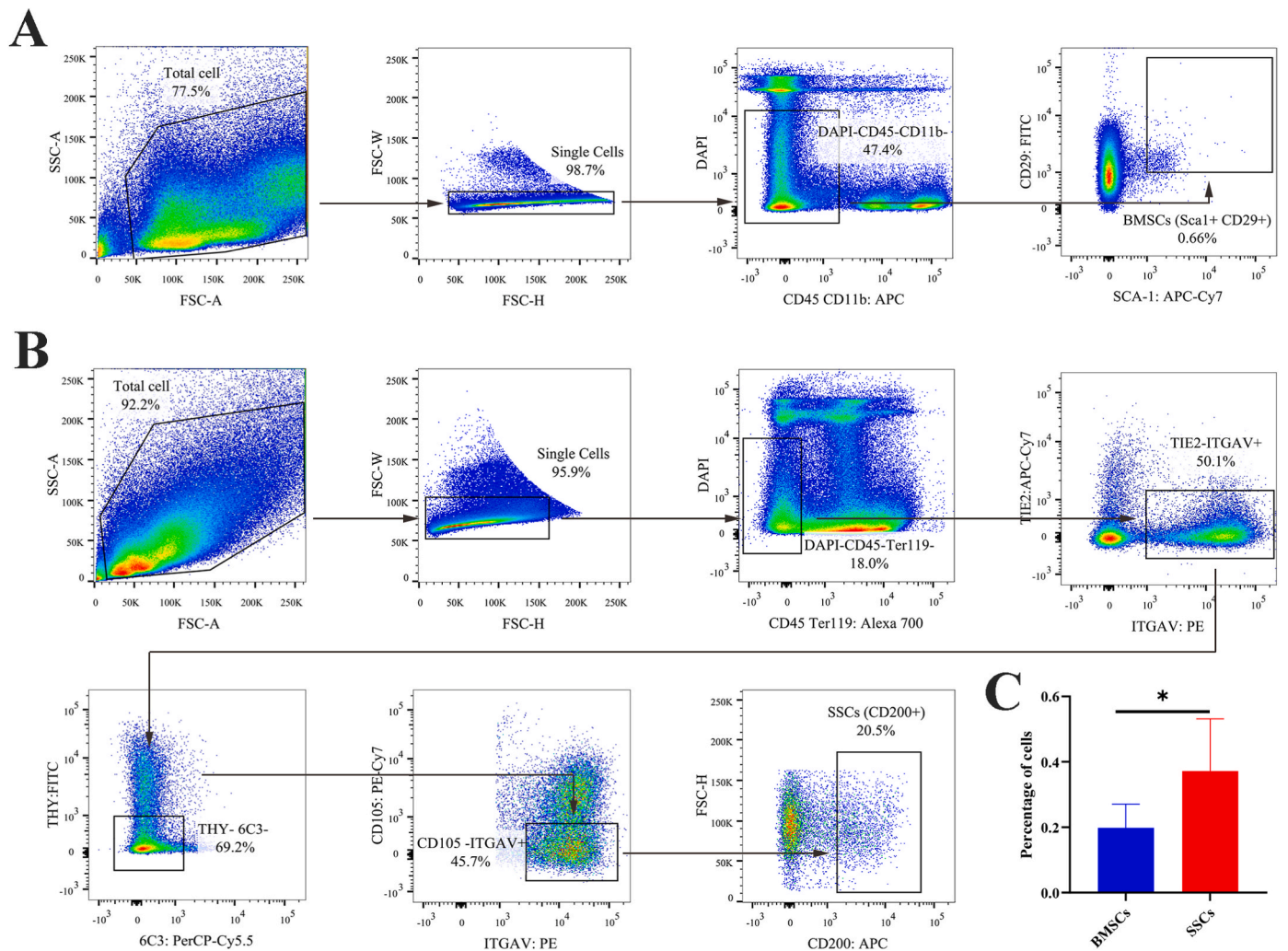
Fig. 1. Fluorescence-activated cell sorting for BMSCs and SSCs. (A) Representative flow cytometry plots gating strategy for isolation of BMSCs. (B) Representative flow cytometry plots gating strategy for isolation of SSCs. (C) Quantification of flow cytometry data of the sorted cells. n = 6 per group. Data are represented as mean ± SD, *p < 0.05 represent significant differences between the indicated columns.

decalcified in EDTA, dehydrated in gradient ethanol, and embedded in paraffin. The 5 μm of paraffin sections were deparaffinized, rehydrated, and stained with hematoxylin and eosin (H&E) and toluidine blue &fast green staining (TB&FG) to examine the characteristics of repaired TBI. The semi-quantitative analysis of histological staining was carried out by two observers who were unaware of the group allocation and time by using a previously reported modified tendon maturation rating score [30,31]. The specific enthesis area chosen for histological assessment was determined according to a previous similar study [32].

2.6. Micro-computed tomography (Micro-CT)

All samples were fixed in 4 % paraformaldehyde and scanned with Micro-CT system (Hiscan XM, China) to evaluate new bone formation at ST enthesis. Imaging was performed with 10 μm isotropic voxel size, 10 μm spatial resolution, and 500 ms exposure time at 60 kV/134 μA. The three-dimensional images of humeral head were reconstructed by Amira (Visage Imaging, Australia). Additionally, morphometric parameters in the region of interest, including bone volume/total volume (BV/TV), trabecular number (Tb. N), trabecular thickness (Tb. Th), and trabecular separation (Tb. Sp), were calculated using CT-Analyzer (CTAn, Bruker, Germany). The selected region of interest for the analysis was based on previous recommendations [32–34], encompassing the trabecular bone within the humeral head near the tendon insertion and proximal to the growth plate.

2.7. Biomechanical testing

A biomechanical testing system (Instron, Boston, USA) was used to determine the failure load, ultimate stress, stiffness, and distance of repaired ST enthesis. Additionally, intact normal specimens that did not undergo surgery served as a reference to assess the extent of recovery of the mechanical properties of the injured TBI. To calculate cross-sectional area (CSA), the width and thickness of TBI were measured by a vernier caliper before the test. The ST was then secured in the upper clamp, while the humerus shaft was firmly clamped by a lower one, and the specimen was positioned for uniaxial tensile testing at an abduction angle of 60°. Finally, the specimens were preconditioned with 0.1 N and then loaded at a rate of 0.1 mm/s until the attached tendon ruptured or failed at the repaired site. The failure load, distance, and stiffness were extracted from the load–deformation curves, while the ultimate stress was computed as the maximum load the sample could endure divided by the CSA.

2.8. Statistical analysis

Data were expressed as mean ± standard deviation and analyzed by using GraphPad Prism software. The independent-sample t-test or one-
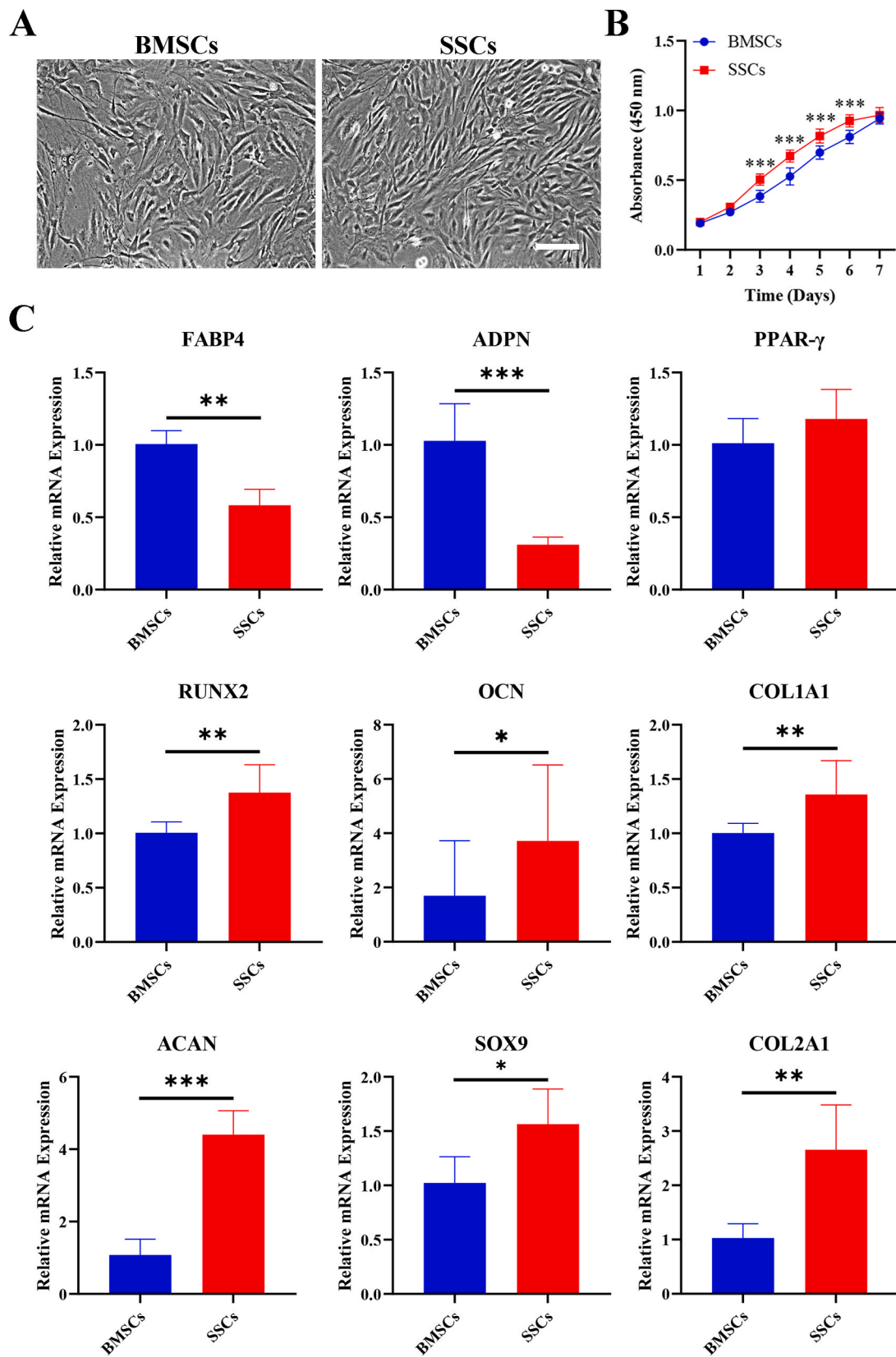
Fig. 2. Cellular characterization of BMSCs and SSCs. (A) Representative morphology of BMSCs and SSCs. Scale bar: 200 μm; (B) Proliferative capacity of BMSCs and SSCs evaluated by Cell Counting Kit-8 (CCK-8) assays from day 1 to day 7. n = 6 per group. (C) qRT-PCR analysis for the expression of adipogenic gene (FABP4, ADPN, and PPAR-γ), osteogenic gene (RUNX2, OCN, and COL1A1) and chondrogenic gene (ACAN, SOX9, and COL2A1) in BMSCs and SSCs. n = 6 per group. Data are represented as mean ± SD, *p < 0.05, **p < 0.01, ***p < 0.001 represent significant differences between the indicated columns.
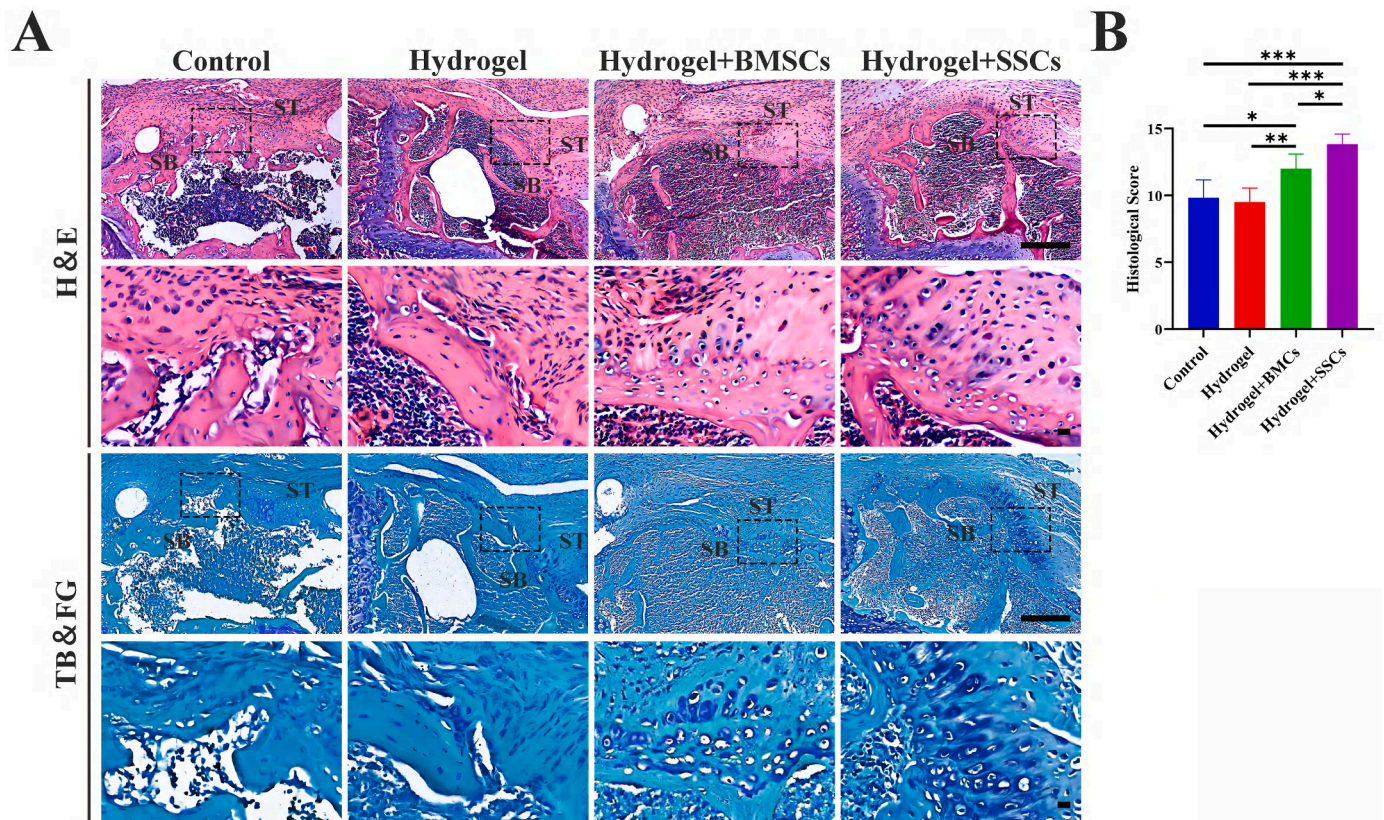
Fig. 3. Histologic evaluation of ST enthesis at 4 weeks postoperatively. (A) Representative images of H&E and TB&FG staining at the repaired site. The area selected by the rectangle dashed line is the local magnified area. scale bar = 200 μm; (B) Tendon-to-bone insertion maturing score of regenerated enthesis. n = 6 per group. ST, supraspinatus tendon; H&E, hematoxylin and eosin; TB&FG, toluidine blue and fast green; All data are mean ± SD. *p < 0.05, **p < 0.01, ***p < 0.001 represent significant differences between the indicated columns. (For interpretation of the references to colour in this figure legend, the reader is referred to the Web version of this article.)

way analysis of variance (ANOVA) followed by Tukey's post hoc test was performed to evaluate the difference in data at a single time point. The two-way ANOVA followed by Tukey's post hoc test was performed to evaluate the difference of data at multiple time points. P < 0.05 indicated a significant statistical difference.

3. Results

3.1. Isolation of BMSCs and SSCs by flow cytometry

Lived SSCs were successfully obtained from the femur and tibia by flow cytometry with positive markers ITGAV and CD200 but negative markers DAPI, CD45, Ter119, TIE2, THY, 6C3, and CD105. Similarly, lived BMSCs were also sorted from bone marrow by flow cytometry with positive markers SCA-1 and CD29 but negative markers DAPI, CD45, and CD11b. Interstingly, quantification of cellular frequency of FACS demonstrated that the SSCs have a higher proportion than BMSCs (P < 0.05) (Fig. 1).

3.2. Characterization of BMSCs and SSCs

After the primary culture, both SSCs and BMSCs exhibited spindle-shaped and fibroblast-like morphology (Fig. 2A). Next, cell proliferation was measured daily for 7 days by using a CCK-8 kit. Based on Fig. 2B, SSCs had stronger proliferation capacity than BMSCs from day 3–6 after seed (P < 0.05). For trilineage differentiation potential, qRT-PCR was performed to detect the expression levels of various adipogenic, osteogenic, and chondrogenic factors in SSCs and BMSCs (Fig. 2C). When compared to BMSCs, SSCs had significantly higher

mRNA expression levels of the chondrogenic and the osteogenic genes (P < 0.05). However, the basal expression levels of specific adipogenic markers such as FABP4 and ADPN were lower in SSCs than BMSCs (P < 0.05) but no significant difference was noted in the expression levels of PPAR-γ between them (P > 0.05).

3.3. Histological evaluation

H&E and TB&FG staining were used for histological evaluation of the regenerated enthesis in each group. At 4 and 8 weeks after surgery, the TBI area in hydrogel + SSCs group showed better organizational continuity, more chondrocytes, larger areas of glycosaminoglycan staining, fewer infiltrating inflammatory cells, and higher modified tendon-to-bone maturity scores (P < 0.05) than those of the other three groups. The results of histological assessments demonstrated that the transplantation of SSCs was more beneficial for the formation of mature TBI in the mice RC repair model when compared to BMSCs, which highlighted the application of SSCs for TBI injury (Figs. 3 and 4).

3.4. Micro-CT analysis

Based on representative three-dimensional reconstruction of Micro-CT images for humeral head, bone loss was observed at injured site and bone volume continued to increase with healing time among all groups (Fig. 5A). Quantitatively, microarchitectural parameter analysis showed that the BV/TV and Tb. N of newly formed bone were the highest in the hydrogel + SSCs group among the four groups at 8 weeks postoperatively (P < 0.05). Tb. Sp levels were significantly lower in the hydrogel + SSCs group than that in hydrogel and hydrogel + BMSCs
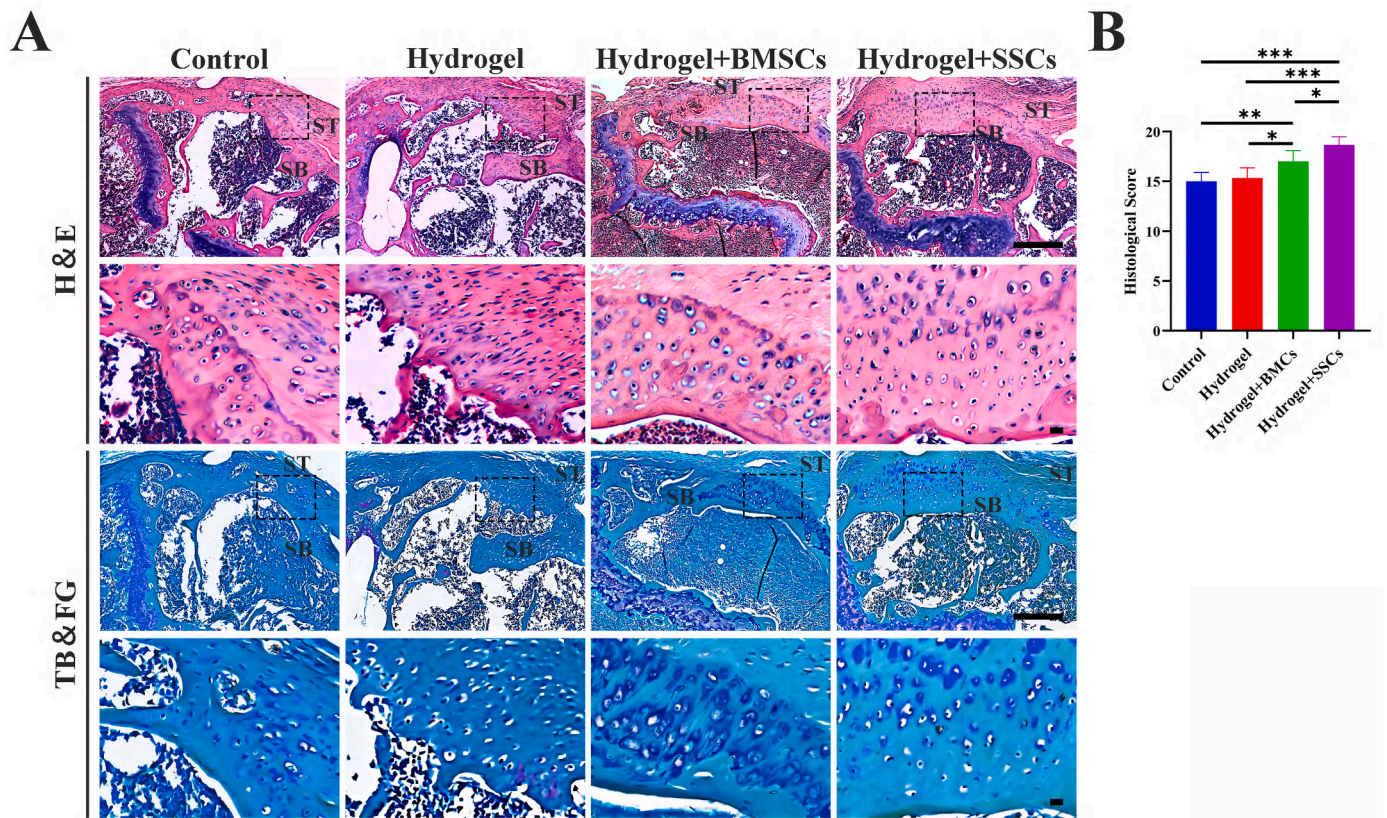
Fig. 4. Histologic evaluation of ST enthesis at 8 weeks postoperatively. (A) Representative images of H&E and TB&FG staining at the repaired site. The area selected by the rectangle dashed line is the local magnified area. scale bar = 200 μm. (B) Tendon-to-Bone insertion maturing score of the regenerated enthesis. n = 6 per group. ST, supraspinatus tendon; H&E, hematoxylin and eosin; TB&FG, toluidine blue and fast green; All data are mean ± SD. *p < 0.05, **p < 0.01, ***p < 0.001 represent significant differences between the indicated columns. (For interpretation of the references to colour in this figure legend, the reader is referred to the Web version of this article.)

group at 4 weeks postoperatively (P < 0.05). Moreover, hydrogel + SSCs and hydrogel + BMSCs groups had significantly higher BV/TV at 4 and 8 weeks postoperatively and lower Tb. Sp at 8 weeks postoperatively when compared with control and hydrogel groups (P < 0.05). These results indicate that higher quality of new bone was formed at the tendon-bone interface in the hydrogel + SSCs group as compared to that in the other three groups (Fig. 5B).

3.5. Biomechanical test

In biomechanical testing, all failures occurred at the ST insertion site. At 4 and 8 weeks after surgery, the hydrogel + SSCs groups exhibited higher failure load, ultimate stress, and stiffness compared to the control groups or the blank hydrogel group (P < 0.05). Additionally, the ultimate stress at 4 weeks postoperatively in the hydrogel + BMSCs groups was higher than that in the control group (P < 0.05), and the ultimate stress at 8 weeks postoperatively in the hydrogel + SSCs groups was higher than that in the hydrogel + BMSCs groups (P < 0.05). There were no differences in the distance of repaired enthesis among the four groups at weeks 4 and 8 postoperatively (P > 0.05), and no difference in failure load, ultimate stress, and stiffness were observed between the control and hydrogel groups at 4 and 8 weeks postoperatively (P > 0.05). These results indicated that the SSCs would augment the biomechanical properties of regenerated TBI better than BMSCs (Fig. 6).

### 3.6. Gene expression analysis for repaired ST enthesis

At 4 or 8 weeks after surgery, the qRT-PCR results (Fig. 7) demonstrated a significant upregulation in the expression of osteogenic genes

(Runx2, OCN, and COL1A1) and chondrogenic genes (ACAN, SOX9, and COL2A1) within the healing interface tissues in the hydrogel + SSCs group compared to the control groups or blank hydrogel group (P < 0.05). Moreover, the expression of COL1A1, ACAN and SOX9 at 4 weeks postoperatively was significantly higher in the hydrogel + SSCs group compared to the hydrogel + BMSCs group. These findings suggested SSCs may exhibit superior effectiveness over BMSCs in promoting osteogenesis and chondrogenesis at the injured ST enthesis.

4. Discussion

In this study, we intend to compare the therapeutic potential of SSCs and BMSCs on tendon enthesis regeneration following acute rotator cuff injury, thereby optimizing original cell therapy for T-B healing. Therefore, we first successfully isolated both types of stem cells and observed that the proportion of SSCs within the femur and tibia was higher compared to the proportion of BMSCs in the bone marrow. Next, we confirmed that SSCs showed stronger ability for proliferation, osteogenesis, chondrogenesis, and lower adipogenesis capacity than BMSCs while SSCs had a similar shape as BMSCs. Furthermore, our result verified the hypothesis that SSCs would enhance T-B healing than BMSCs, as evidenced by more new bone formation, superior histological morphology, greater biomechanical properties, and higher expression of osteogenic and chondrogenic genes at TBI in SSCs group when compared with the other three groups.

Achieving the regenerated enthesis with better biomechanical properties and more mature tissue formation has always been a great challenge in sports medicine [35–37]. Attributing to the importance of the biological environment during healing, cell-based therapies have
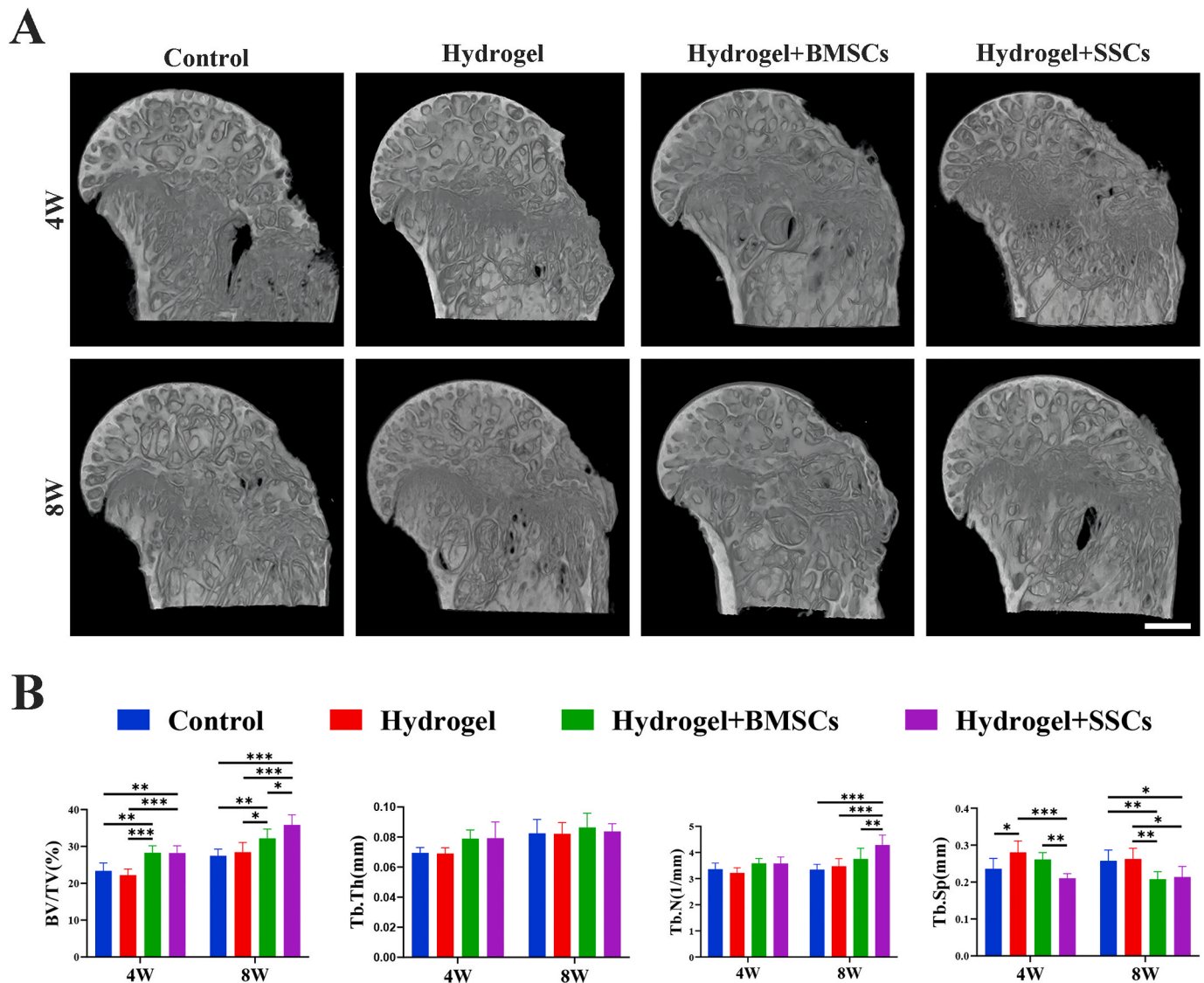
Fig. 5. Radiological analysis by Micro-CT for RC healing site at 4 and 8 weeks postoperatively. (A) three-dimensional reconstruction image of the humeral head, Scale bar = 500 μm. (B) The morphological parameters of new bone at the healing site. n = 6 per group. RC, rotator cuff; BV/TV, bone volume/total volume; Tb.Th, trabecular thickness; Tb.N, trabecular number; Tb.Sp, trabecular separation. All data are mean ± SD. *p < 0.05, **p < 0.01, ***p < 0.001 represent significant differences between the indicated columns.

attracted increasing attention within regenerative musculoskeletal medicine [38–40]. The generally used cell types that are applicable in promoting enthesis regeneration include terminally differentiated cells like osteoblasts and various kinds of stem cells [11,41]. MSCs may be more appealing for the enhancement of T-B healing than differentiated cells due to their ease of isolation and culture, high rate of proliferation, and multilineage differentiation in response to local signals [15]. Among MSCs from different sources, BMSCs have been explored the most [16, 42]. At present, tissue engineering researchers have been committed to find seed cells that are more suitable than BMSCs to promote bone healing. Recent studies have revealed that synovium-derived mesenchymal stem cells (SMSCs), periosteum-derived periosteal stem cells (PSCs), and tendon-derived stem/progenitor cells (TSPCs) exhibit higher capacities for proliferation, osteogenic differentiation, and chondrogenic differentiation compared to BMSCs. However, the isolation of these stem cells requires invasive surgical procedures to obtain the appropriate tissue [14,43]. On the other hand, adipose-derived mesenchymal stem cells (ADSCs) can be easily harvested from the fat of most animals and humans and possess a stronger proliferative ability. However, they have lower osteogenic and chondrogenic potential compared

to BMSCs [14,44]. The limited sources of SMSCs, PSCs, and TSPCs, as well as the relatively poor osteogenic and chondrogenic differentiation abilities of ADSCs, currently restrict their clinical implementation, especially in the context of TBI repairs.

SSCs, a skeletogenic cells, could be identified and isolated from long bones, bone marrow, mandibles, cranial sutures, and BMP2-treated adipose [22,23,45]. Interestingly, our result confirmed for the first time that we could obtain higher proportion of SSCs in long bones when compared to the isolation of BMSCs from bone marrow. Given that SSCs are upstream stem cells of skeletal lineage, we hypothesized that SSCs have strong ability with proliferation and skeletogenic differentiation. To validate our hypothesis, we conducted a series of functional assays to compare SSCs and the most applied seed cell, BMSCs. We found that SSCs have stronger multiplication capacity than BMSCs. Moreover, the results of qRT-PCR showed that the expression of the osteogenic and chondrogenic makers of SSCs was higher, and adipogenic markers were lower than BMSCs. These findings provided the theoretical basis for in vivo application of SSCs in the present study.

The main concern of this study is whether SSCs have the potential to promote the regeneration of a physiological enthesis in murine rotator
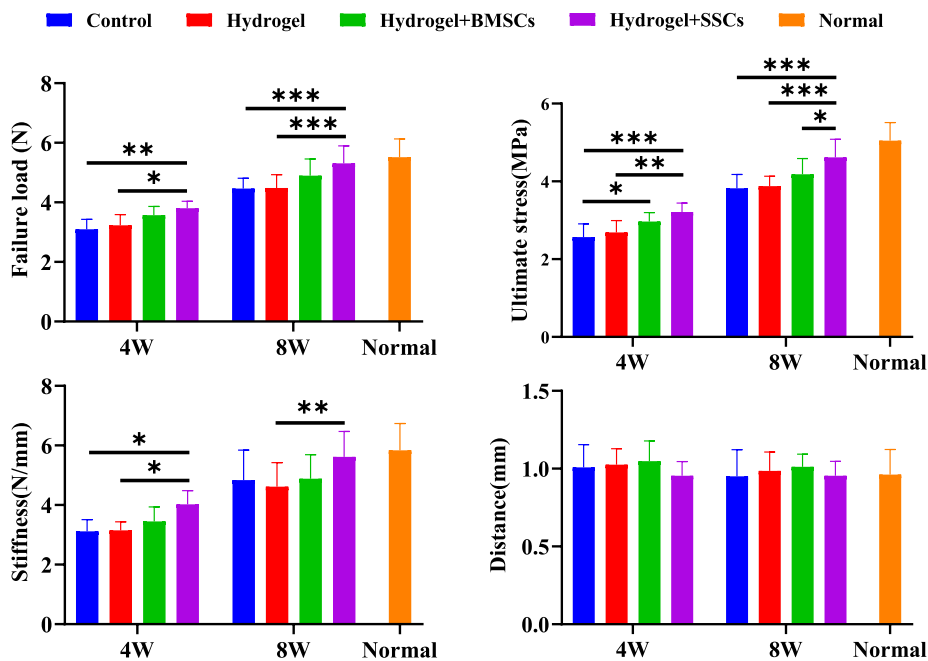
Fig. 6. Biomechanical testing for the insertion site of supraspinatus tendon–humerus complexes at postoperative weeks 4 and 8, as expressed by failure load, stiffness, ultimate stress, and cross-sectional area. n = 10 per group. Data are represented as mean ± SD, *p < 0.05, **p < 0.01, ***p < 0.001 represent significant differences between the indicated columns.
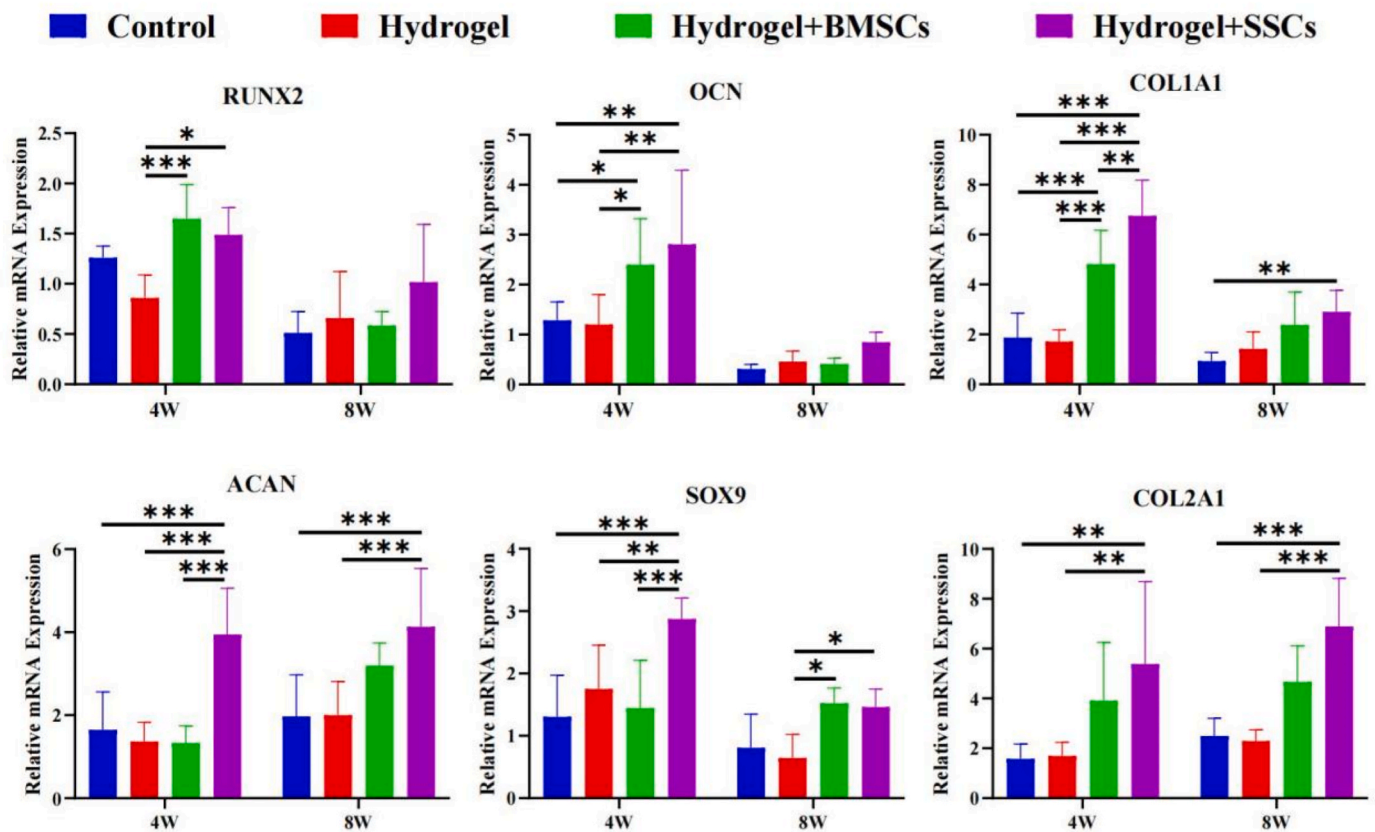

Fig. 7. qRT-PCR analysis for the expression of osteogenic gene (RUNX2, OCN, and COL1A1) and chondrogenic gene (ACAN, SOX9, and COL2A1) in the mouse ST enthesis after injury-repair surgery. n = 6 per group. The fold change of expression was determined by comparing the expression level of repaired ST enthesis in different treatment groups to that in the normal enthesis. The data are presented as mean ± SD. *p < 0.05, **p < 0.01, ***p < 0.001 represent significant differences between the indicated columns. ST, supraspinatus tendon.

cuff repair model. The quality of T-B healing could be determined in various manners. For example, histological staining and Micro-CT scanning were performed to determine the structural characteristics of repaired TBI like chondrogenesis and osteogenesis [10,46]. The expression of chondrogenic and osteogenic genes in healing interface tissue could be further detected by qRT-PCR. Moreover, biomechanical property was regarded as ultimate criterion to assess T-B healing and was closely associated with the failure rate of reconstruction surgery [29,47,48]. Based on all findings in this study, we concluded that the transplantation of SSCs resulted in higher chondrogenesis, osteogenesis, and biomechanical properties at regenerated enthesis as compared with BMSCs, which provided a better cell-based strategy for TBI injury.

There were some limitations in this study. First, most rotator cuff tears in a clinic are chronic, however, this study was performed in an acute injury model. Therefore, comparison of therapeutic effects between SSCs and BMSCs on T-B healing should best be revalidated in a chronic rotator cuff tear model. Second, we isolated SSCs and BMSCs from mice. To advance the clinical application of SSCs, further studies might be conducted to compare the therapeutic efficacy of human SSCs and BMSCs on TBI regeneration. Third, considering the significant difference in T-B healing rate between humans and mice, this study could be repeated on a larger animal model such as the dog or pig.

5. Conclusion

In summary, SSCs exhibited stronger proliferation capacity, expressed higher chondrogenic and osteogenic markers, and showed more effective therapeutic effects on TBI injury than BMSCs. Our findings suggest that SSCs might be a better cell source than BMSCs for the promotion of T-B healing.

Declaration of competing interest

All experimental procedures were approved by our institutional Animal Care and Use Committees (No. 2022020058). The authors do not have any conflicts of interest relevant to the publication of this paper.

Funding

Author contributions

H.L. and J.H. conceived and designed study. L.W. and C.G. performed experiments. C.G. and Y.L. analyzed data. L.W. drafted the original manuscript. D.X., T.Z. and Y.Z. revised the manuscript and assisted in data analysis.

Acknowledgments

Appendix A. Supplementary data

Supplementary data to this article can be found online at https://doi.org/10.1016/j.jot.2024.05.005.

References

[1] Fang F, Xiao Y, Zelzer E, Leong KW, Thomopoulos S. A mineralizing pool of Gli1-expressing progenitors builds the tendon enthesis and demonstrates therapeutic potential. Cell Stem Cell 2022;29(12) [eng].

[2] Zhang T, Li S, Chen Y, Xiao H, Wang L, Hu J, et al. Characterize the microstructure change after tendon enthesis injury using synchrotron radiation μCT. J Orthop Res 2022;40(11):2678–87 [eng].

[3] Zhou Y, Xie S, Tang Y, Li X, Cao Y, Hu J, et al. Effect of book-shaped acellular tendon scaffold with bone marrow mesenchymal stem cells sheets on bone-tendon interface healing. J Orthop Translat 2021;26:162–70 [eng].

[4] Xiao H, Zhang T, Li CJ, Cao Y, Wang LF, Chen HB, et al. Mechanical stimulation promotes enthesis injury repair by mobilizing cells via ciliary TGF-β signaling. Elife 2022;11 [eng].

[5] Yea J-H, Bae TS, Kim BJ, Cho YW, Jo CH. Regeneration of the rotator cuff tendon-to-bone interface using umbilical cord-derived mesenchymal stem cells and gradient extracellular matrix scaffolds from adipose tissue in a rat model. Acta Biomater 2020;114:104–16 [eng].

[6] Zhang J, Liu Z, Tang J, Li Y, You Q, Yang J, et al. Fibroblast growth factor 2-induced human amniotic mesenchymal stem cells combined with autologous platelet rich plasma augmented tendon-to-bone healing. J Orthop Translat 2020; 24:155–65 [eng].

[7] Zhang T, Yan S, Song Y, Chen C, Xu D, Lu B, et al. Exosomes secreted by hypoxia-stimulated bone-marrow mesenchymal stem cells promote grafted tendon-bone tunnel healing in rat anterior cruciate ligament reconstruction model. J Orthop Translat 2022;36:152–63 [eng].

[8] Wang L, Jiang J, Lin H, Zhu T, Cai J, Su W, et al. Advances in regenerative sports medicine research. Front Bioeng Biotechnol 2022;10:908751 [eng].

[9] Chen Y, Xu Y, Li M, Shi Q, Chen C. Application of autogenous urine-derived stem cell sheet enhances rotator cuff healing in a canine model. Am J Sports Med 2020; 48(14):3454–66 [eng].

[10] Chen W, Sun Y, Gu X, Cai J, Liu X, Zhang X, et al. Conditioned medium of human bone marrow-derived stem cells promotes tendon-bone healing of the rotator cuff in a rat model. Biomaterials 2021;271:120714.

[11] Luo W, Wang Y, Han Q, Wang Z, Jiao J, Gong X, et al. Advanced strategies for constructing interfacial tissues of bone and tendon/ligament. J Tissue Eng 2022;13: 20417314221144714 [eng].

[12] Rohman ML, Snow M. Use of biologics in rotator cuff disorders: current concept review. J Clin Orthop Trauma 2021;19:81–8 [eng].

[13] Atesok K, Fu FH, Wolf MR, Ochi M, Jazrawi LM, Doral MN, et al. Augmentation of tendon-to-bone healing. J Bone Joint Surg Am 2014;96(6):513–21 [eng].

[14] Xu Y, Zhang W-X, Wang L-N, Ming Y-Q, Li Y-L, Ni G-X. Stem cell therapies in tendon-bone healing. World J Stem Cell 2021;13(7):753–75 [eng].

[15] Lei T, Zhang T, Ju W, Chen X, Heng BC, Shen W, et al. Biomimetic strategies for tendon/ligament-to-bone interface regeneration. Bioact Mater 2021;6(8): 2491–510 [eng].

[16] Wang C, Hu Y, Zhang S, Ruan D, Huang Z, He P, et al. Application of stem cell therapy for ACL graft regeneration. Stem Cell Int 2021;2021:6641818 [eng].

[17] Yang C, Teng Y, Geng B, Xiao H, Chen C, Chen R, et al. Strategies for promoting tendon-bone healing: current status and prospects. Front Bioeng Biotechnol 2023; 11:1118468 [eng].

[18] Chen P, Cui L, Fu SC, Shen L, Zhang W, You T, et al. The 3D-printed PLGA scaffolds loaded with bone marrow-derived mesenchymal stem cells augment the healing of rotator cuff repair in the rabbits. Cell Transplant 2020;29:963689720973647 [eng].

[19] Chan CKF, Seo EY, Chen JY, Lo D, McArdle A, Sinha R, et al. Identification and specification of the mouse skeletal stem cell. Cell 2015;160(1–2):285–98 [eng].

[20] Baek I, Bello AB, Jeon J, Arai Y, Cha B-H, Kim BJ, et al. Therapeutic potential of epiphyseal growth plate cells for bone regeneration in an osteoporosis model. J Tissue Eng 2022;13:20417314221116754 [eng].

[21] Papageorgiou P, Vallmajo-Martin Q, Kisielow M, Sancho-Puchades A, Kleiner E, Ehrbar M. Expanded skeletal stem and progenitor cells promote and participate in induced bone regeneration at subcritical BMP-2 dose. Biomaterials 2019;217: 119278 [eng].

[22] Murphy MP, Koepke LS, Lopez MT, Tong X, Ambrosi TH, Gulati GS, et al. Articular cartilage regeneration by activated skeletal stem cells. Nat Med 2020;26(10): 1583–92 [eng].

[23] Titan AL, Davitt M, Foster D, Salhotra A, Menon S, Chen K, et al. Partial tendon injury at the tendon-to-bone enthesis activates skeletal stem cells. Stem Cells Transl Med 2022;11(7):715–26 [eng].

[24] Sakaguchi Y, Sekiya I, Yagishita K, Muneta T. Comparison of human stem cells derived from various mesenchymal tissues: superiority of synovium as a cell source. Arthritis Rheum 2005;52(8):2521–9 [eng].

[25] Zuo R, Liu J, Zhang Y, Zhang H, Li J, Wu J, et al. In situ regeneration of bone-to-tendon structures: comparisons between costal-cartilage derived stem cells and BMSCs in the rat model. Acta Biomater 2022;145:62–76 [eng].

[26] Su T, Xiao Y, Xiao Y, Guo Q, Li C, Huang Y, et al. Bone marrow mesenchymal stem cells-derived exosomal MiR-29b-3p regulates aging-associated insulin resistance. ACS Nano 2019;13(2):2450–62 [eng].

[27] Tang Y, Wu X, Lei W, Pang L, Wan C, Shi Z, et al. TGF-beta1-induced migration of bone mesenchymal stem cells couples bone resorption with formation. Nat Med 2009;15(7):757–65 [eng].

[28] Marecic O, Tevlin R, McArdle A, Seo EY, Wearda T, Duldulao C, et al. Identification and characterization of an injury-induced skeletal progenitor. Proc Natl Acad Sci USA 2015;112(32):9920–5 [eng].

[29] Liu Y, Wang L, Li S, Zhang T, Chen C, Hu J, et al. Mechanical stimulation improves rotator cuff tendon-bone healing via activating IL-4/JAK/STAT signaling pathway mediated macrophage M2 polarization. J Orthop Translat 2022;37:78–88 [eng].

[30] Zhang T., Chen Y., Chen C., Li S., Xiao H., Wang L., et al. Treadmill exercise facilitated rotator cuff healing is coupled with regulating periphery neuropeptides expression in a murine model. J Orthop Res 2021;39(3):680-692.[eng].

[31] Chen Y, Zhang T, Wan L, Wang Z, Li S, Hu J, et al. Early treadmill running delays rotator cuff healing via Neuropeptide Y mediated inactivation of the Wnt/β-catenin signaling. J Orthop Translat 2021;30:103–11 [eng].

[32] Shah SA, Kormpakis I, Havlioglu N, Ominsky MS, Galatz LM, Thomopoulos S. Sclerostin antibody treatment enhances rotator cuff tendon-to-bone healing in an animal model. J Bone Joint Surg Am 2017;99(10):855–64 [eng].

[33] Xu J, Ye Z, Chen C, Zhang X, Han K, Wu X, et al. Abaloparatide improves rotator cuff healing via anabolic effects on bone remodeling in a chronic rotator cuff tear model of rat with osteoporosis: a comparison with denosumab. Am J Sports Med 2022;50(6):1550–63 [eng].

[34] Xu J, Su W, Chen J, Ye Z, Wu C, Jiang J, et al. The effect of antiosteoporosis therapy with risedronate on rotator cuff healing in an osteoporotic rat model. Am J Sports Med 2021;49(8):2074–84 [eng].

[35] Song W, Ma Z, Wang C, Li H, He Y. Pro-chondrogenic and immunomodulatory melatonin-loaded electrospun membranes for tendon-to-bone healing. J Mater Chem B 2019;7(42):6564–75 [eng].

[36] Li Y, Zhou M, Zheng W, Yang J, Jiang N. Scaffold-based tissue engineering strategies for soft-hard interface regeneration. Regen Biomater 2023;10:rbac091 [eng].

[37] Han F, Li T, Li M, Zhang B, Wang Y, Zhu Y, et al. Nano-calcium silicate mineralized fish scale scaffolds for enhancing tendon-bone healing. Bioact Mater 2023;20: 29–40 [eng].

[38] Özdemir E, Karaguven D, Turhan E, Huri G. Biological augmentation strategies in rotator cuff repair. Med Glas 2021;18(1):186–91 [eng].

[39] Davies M, T Feeley B. Editorial commentary: stem cell exosomes can promote healing and muscle function after rotator cuff repair. Arthroscopy 2022;38(7): 2154–6 [eng].

[40] Mirzayan R, Weber AE, Petrigliano FA, Chahla J. Rationale for biologic augmentation of rotator cuff repairs. J Am Acad Orthop Surg 2019;27(13):468–78 [eng].

[41] Roßbach BP, Gülecyüz MF, Kempfert L, Pietschmann MF, Ullamann T, Ficklscherer A, et al. Rotator cuff repair with autologous tenocytes and biodegradable collagen scaffold: a histological and biomechanical study in sheep. Am J Sports Med 2020;48(2):450–9 [eng].

[42] Zhang J, Liu Z, Li Y, You Q, Yang J, Jin Y, et al. FGF-2-Induced human amniotic mesenchymal stem cells seeded on a human acellular amniotic membrane scaffold accelerated tendon-to-bone healing in a rabbit extra-articular model. Stem Cell Int 2020;2020:4701476 [eng].

[43] Burk J, Ribitsch I, Gittel C, Juelke H, Kasper C, Staszyk C, et al. Growth and differentiation characteristics of equine mesenchymal stromal cells derived from different sources. London, England Vet J 2013;195(1):98–106 [eng].

[44] Chen Y, Xu Y, Dai G, Shi Q, Duan C. Enhanced repaired enthesis using tenogenically differentiated adipose-derived stem cells in a murine rotator cuff injury model. Stem Cell Int 2022;2022:1309684 [eng].

[45] Chan CKF, Gulati GS, Sinha R, Tompkins JV, Lopez M, Carter AC, et al. Identification of the human skeletal stem cell. Cell 2018;175(1):43–56.e21 [eng].

[46] Ye C, Zhang W, Wang S, Jiang S, Yu Y, Chen E, et al. Icariin promotes tendon-bone healing during repair of rotator cuff tears: a biomechanical and histological study. Int J Mol Sci 2016;17(11) [eng].

[47] Chen H, Li S, Xiao H, Wu B, Zhou L, Hu J, et al. Effect of exercise intensity on the healing of the bone-tendon interface: a mouse rotator cuff injury model study. Am J Sports Med 2021;49(8):2064–73 [eng].

[48] Zhang M, Deng L, Zhou J, Liu T, Yang Z, Liu J, et al. Combination of autologous osteochondral and periosteum transplantation effectively promotes fibrocartilage regeneration at the tendon-bone junction of the rotator cuff in rabbits. Knee Surg Sports Traumatol Arthrosc 2023;31(5):1953-1962 [eng].